Sedimentary Evolution and Reservoir Formation of the Late Triassic Bolila Formation in the Central Qiangtang Basin, Tibet

Shangke Xie *, Haisheng Yi *, Wangzhong Zhan , Wei Sun , Shengqiang Zeng , Qian Hou , Keyu Zhu

Posted Date: 5 May 2026

doi: 10.20944/preprints202605.0178.v1

Keywords: Qiangtang Basin; Bolila Formation; Late Triassic; sedimentary evolution; reservoir formation

 doi:10.20944/preprints202605.0178.v1

Article

Sedimentary Evolution and Reservoir Formation of the Late Triassic Bolila Formation in the Central Qiangtang Basin, Tibet

Shangke Xie [1,2,*], Haisheng Yi [2,*], Wangzhong Zhan [2], Wei Sun [2], Shengqiang Zeng [2], Qian Hou [2] and Keyu Zhu [2]

[1] Institute of Sedimentary Geology, Chengdu University of Technology, Chengdu 610059, China

[2] Chengdu Geological Survey Center, China Geological Survey (Southwest Geological Science and Technology Innovation Center), Chengdu 610218, China

* Correspondence: shangk86@163.com (S.X.); yhs@cdut.edu.cn (H.Y.)

Abstract

The Late Triassic Bolila Formation in the central Qiangtang Basin is a critical carbonate succession, yet its depositional age and reservoir-forming mechanisms have long been contentious. This study presents an integrated sedimentological, detrital zircon U–Pb geochronological, carbon-oxygen isotopic, and reservoir petrological investigation of the Quemudongda section. Detrital zircon ages constrain the deposition to 225.7–235.7 Ma (Carnian–Norian), correcting its previous Jurassic assignment. Stable carbon and oxygen isotope signatures ($\delta^{13}C$ up to +4.0‰, $\delta^{18}O$ as low as –14.3‰) corroborate the Late Triassic age and indicate a warm, humid paleoenvironment. The section reveals a steep-rimmed platform-margin association dominated by hexactinellid-calcareous sponge reefs intercalated with seven slump-breccia layers, recording three evolutionary stages from reef initiation to decline. Reservoir properties are controlled by the interplay of sedimentation, dolomitization, and fracturing. Early dolomitization generated intercrystalline porosity, but subsequent high-temperature burial recrystallization produced xenotopic textures that severely reduced matrix porosity (average 2.8%). Tectonic microfractures provide the main permeability pathways (0.001–8.5 mD), resulting in a fracture–pore dual-porosity system. Breccia dolostone exhibits significantly better physical properties (average porosity 3.71%, permeability 2.412 mD) than reef dolostone. The platform-margin reef-shoal complex, overlain by Bagong Formation source rocks, forms a favorable lower-reservoir / upper-source assemblage. The breccia dolostone–fracture overlap zone represents the sweet spot for hydrocarbon exploration. These findings offer new insights into carbonate platform-margin evolution and provide a scientific basis for reservoir prediction in the Qiangtang Basin.

Keywords: Qiangtang Basin; Bolila Formation; Late Triassic; sedimentary evolution; reservoir formation

1. Introduction

As the youngest and highest continental plateau on Earth, the Qinghai–Tibet Plateau has profoundly influenced climate dynamics and resource distribution across East Asia and beyond, attracting sustained global geoscientific interest [1,2]. Located in the hinterland of this plateau, the Qiangtang Basin is bounded by the Hoh Xil–Jinshajiang suture zone to the north and the Bangong Co–Nujiang suture zone to the south. It represents the largest Mesozoic marine sedimentary basin in the northern Tethyan–Himalayan tectonic domain. The formation and evolution of this basin are intimately linked to the closure of the Paleo-Tethys Ocean and the subsequent opening of the Neo-Tethys Ocean [3–5]. The basin hosts a thick succession of Triassic–Jurassic marine strata, making it

 doi:10.20944/preprints202605.0178.v1

not only a pivotal area for understanding Tethyan tectonic evolution but also a key strategic frontier for onshore hydrocarbon exploration in China [6–8].

Among the marine strata in the Qiangtang Basin, the Upper Triassic Bolila Formation and the Middle Jurassic Buqu Formation are the two most representative carbonate successions. The Bolila Formation, deposited during the Carnian–Norian stages of the Late Triassic, records a major regional transgression. Its lithology is dominated by carbonate platform limestones and bioclastic limestones, with local reef development, representing the last large-scale carbonate buildup on the northern margin of the Qiangtang block prior to the closure of the Paleo-Tethys Ocean [9–11]. Moreover, the Bolila Formation exhibits considerable hydrocarbon exploration potential due to the presence of platform-margin reef-shoal dolomitized reservoirs [12,13]. However, harsh natural conditions, poor outcrop continuity, complex structural deformation, and inherent limitations of biostratigraphic studies have led to long-standing controversies regarding the stratigraphic division and age assignment of key units in this region [11,14]. Consequently, the sedimentary evolution model and reservoir-forming mechanisms of this formation remain poorly understood.

As an important potential reservoir in the Qiangtang Basin, the Bolila Formation poses several key scientific questions concerning its sedimentary evolution and reservoir formation: (1) What is the precise depositional age of the Bolila Formation, and how can a robust chronostratigraphic framework be established to resolve regional stratigraphic controversies? (2) What sedimentary system does the Bolila Formation represent, and how did the platform-margin reef-shoal system respond to the Late Triassic transgression? (3) What are the formation mechanisms and principal controlling factors of the Bolila Formation reservoirs, and how do dolomitization, dissolution, and fractures contribute to reservoir quality? Addressing these questions is of great scientific significance for reconstructing the Late Triassic paleogeographic framework of the Qiangtang Basin and evaluating its hydrocarbon potential.

This study focuses on the Quemudongda section in the Tuonamu area, which is located in the central part of the North Qiangtang Depression. This section exhibits a complete stratigraphic succession, making it an ideal candidate for investigating the sedimentary evolution and reservoir-forming effects of the Bolila Formation. The following work is systematically carried out: (1) detailed sedimentary facies analysis and microfacies identification to reconstruct the depositional model; (2) detrital zircon U-Pb dating and carbon-oxygen isotope analysis to precisely constrain the depositional age and reconstruct the paleo-marine environment; and (3) reservoir petrology and physical property analysis to reveal pore types, diagenetic processes, and their control on reservoir quality. By integrating these analyses, this study aims to elucidate the sedimentary evolution pattern and reservoir-forming effects of the Bolila Formation, thereby providing a scientific basis for hydrocarbon exploration in the Qiangtang Basin.

2. Regional Geological Setting

The Qiangtang Basin, covering an area of approximately 18×10^4 km^2 in the north-central part of the Qinghai–Tibet Plateau, represents the largest Mesozoic marine sedimentary basin on the plateau [3,15]. It is bounded to the north by the Hoh Xil–Jinshajiang suture zone and to the south by the Bangong Co–Nujiang suture zone, which mark the closure of the Paleo-Tethys and Meso-Tethys oceans, respectively. These sutures collectively underpin the key tectonic role of the Qiangtang Basin in the evolution of the Tethyan realm [1,2,16]. Based on basement nature and sedimentary cover characteristics, the basin can be divided from north to south into three second-order tectonic units: the North Qiangtang Depression, the Central Uplift, and the South Qiangtang Depression [9,17]. The Central Uplift, which strikes nearly east–west, exposes Precambrian metamorphic basement and Paleozoic low-grade metamorphic rocks, and serves as a major tectonic divider between the northern and southern parts of the basin [18]. The study area, the Quemudongda section, is located in the central part of the North Qiangtang Depression, a position that is highly representative for recording Late Triassic sedimentary responses.

 doi:10.20944/preprints202605.0178.v1

The Late Triassic was a critical transitional period in the evolution of the Qiangtang Basin. Under the combined influence of the closure of the Paleo-Tethys Ocean and the opening of the Neo-Tethys Ocean, the basin underwent a fundamental tectonic regime shift: the northern Qiangtang area gradually rose from a foreland basin to a subaerial setting, whereas the southern Qiangtang area shifted from continental to marine sedimentation, resulting in a "paleogeographic inversion" [5,34]. This transition not only controlled the distribution of Late Triassic sedimentary facies but also directly influenced the development and distribution of hydrocarbon source rocks and reservoirs. During the Carnian–Norian stages of the Late Triassic, the Qiangtang block was situated at a low latitude on the northern margin of the Paleo-Tethys Ocean. A warm and humid climate, coupled with regional transgression, gave rise to extensive carbonate platforms [9,13]. In the North Qiangtang Depression, the Bolila Formation was deposited as a typical carbonate buildup, and the high-energy platform-margin facies provided favourable conditions for the growth of reefs and shoals [12].

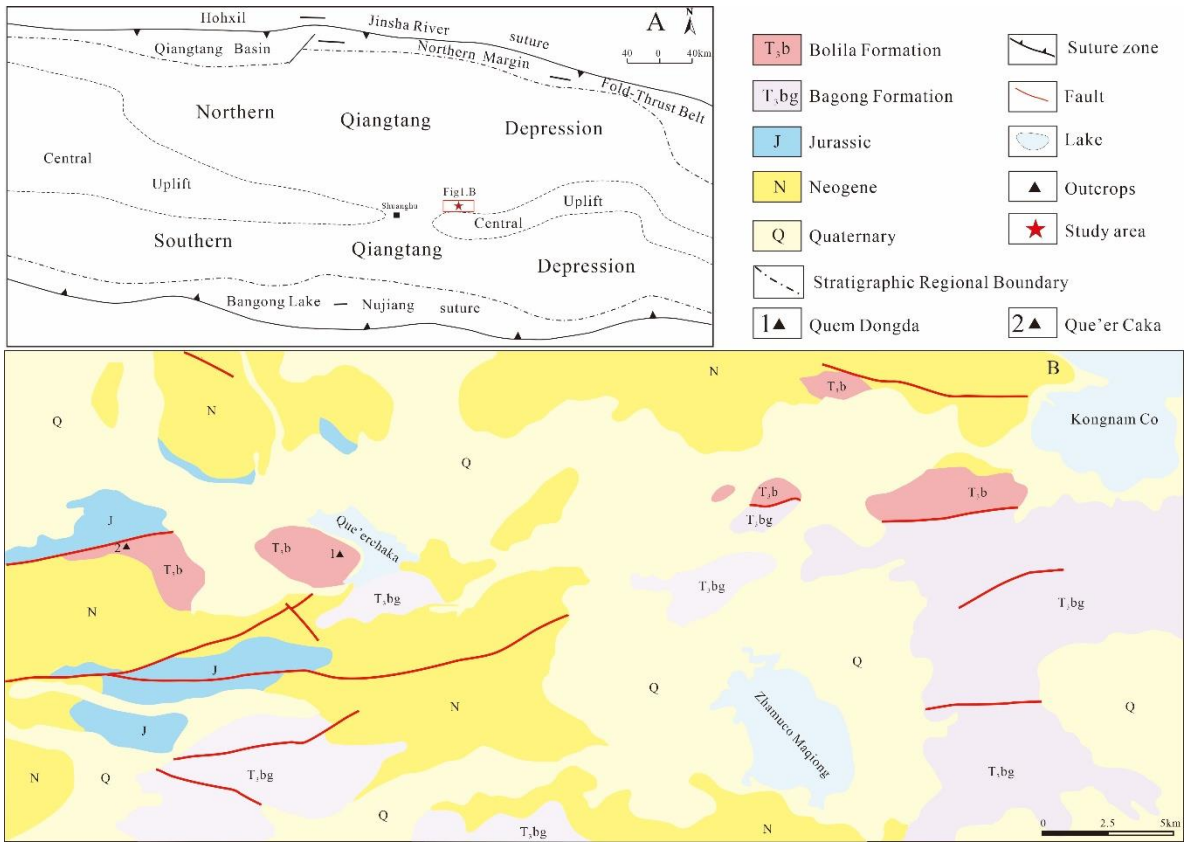

Figure 1. Tectonic units of the Qiangtang Basin and location of the study area.

The Late Triassic strata are well developed in the Qiangtang Basin but exhibit marked differences between the northern and southern parts. In the North Qiangtang Depression, the Upper Triassic succession is divided, from bottom to top, into the Jiapila, Bolila, and Bagong formations, recording a complete transgressive-regressive sedimentary cycle [11]. The Bolila Formation was originally named by the Third Regional Geological Survey Team of Sichuan Province in 1974 from Bolila Mountain in Chagyab County, Tibet, and was originally defined as a set of dark gray to deep gray, medium to thin bedded carbonate rocks intercalated with calcareous mudstones [11]. In the eastern part of the North Qiangtang Depression, the Bolila Formation is dominated by carbonate platform facies, whereas along the northern margin of the Central Uplift, it exhibits typical platform-margin reef–slump breccia associations [12].

During the Carnian–Norian stages, the lithofacies paleogeography of the North Qiangtang Depression was characterized by a "platform–slope–basin" differentiation [19,20]. The inner platform was dominated by open-platform limestones and restricted-platform dolostones, with weak

 doi:10.20944/preprints202605.0178.v1

hydrodynamic conditions. The high-energy platform margin developed reefs and shoals, which constitute the main fairway for high-quality carbonate reservoirs, characterized by well-developed primary porosity and later susceptibility to dolomitization and dissolution. The platform-margin slope zone contains slump breccias and turbidites, recording instability events along the platform margin. The basin facies mainly consist of dark mudstones, shales, and siliceous rocks, representing potential source rock intervals. The Quemudongda section is located in the platform-margin facies belt, and its symbiotic association of reefs and slump breccias provides an ideal opportunity to study the platform-margin depositional system, reservoir development, and source-reservoir-seal configurations.

The Quemudongda section is situated in the Tonam area of Shuanghu County, in the central part of the North Qiangtang Depression. Its geographic coordinates are: starting point N 33°12′20″, E 89°30′58″; ending point N 33°13′05″, E 89°29′58″. The section is approximately 1000 m long and exposes a continuous stratigraphic succession, with the Bolila Formation exceeding 265 m in thickness. The lithology consists mainly of reef limestones and grainstones, interbedded with multiple breccia layers. The underlying Jiapila Formation is composed of purplish red clastic rocks, with which the Bolila Formation is in conformable contact. The overlying Bagong Formation consists of dark gray mudstones, also in conformable contact, indicating a complete stratigraphic sequence. On the 1:250,000 regional geological map, this succession was erroneously assigned to the Middle Jurassic Buqu Formation. However, its distinctive lithological association (reef development and multiple slump breccia layers) differs significantly from the typical stable platform-margin limestones of the Buqu Formation, suggesting a different depositional setting and age, which calls for high-precision geochronological and integrated stratigraphic investigation.

Regionally, the Que'erchaka area near the section has already been confirmed to contain the Upper Triassic Bolila Formation, consisting of gray, medium to thick bedded limestones and bioclastic limestones [21], providing an important reference for regional stratigraphic correlation. In addition, drilling data from well QK-1 have revealed a complete Upper Triassic succession in the hinterland of the North Qiangtang Depression, offering subsurface evidence for the regional correlation of the Bolila Formation [13,22]. This study focuses on the Quemudongda section and integrates stratigraphic correlation along a north-south transect based on the regional seismic grid, aiming to resolve the age controversy of this problematic succession and to unravel its sedimentary evolution and reservoir-forming effects.

3. Materials and Methods

3.1. Fieldwork and Sample Collection

This study focuses on the Quemudongda section. Two north-south transects along the regional seismic grid were deployed for stratigraphic correlation to ensure systematic and regionally representative sampling.

Section measurement: The Quemudongda section was measured in detail at a scale of 1:200. Lithology, sedimentary structures, and fossil assemblages were systematically documented, and rock specimens and oriented samples were collected layer by layer. The total measured thickness is 362.5 m, encompassing 19 natural layers.

Detrital zircon samples: To precisely constrain the depositional age of the carbonate succession, clastic rock samples were collected from the base (below the carbonate succession) and the top (above the carbonate succession). The basal sample (layer 0) is grayish-green fine-grained lithic sandstone, and the top sample (layer 19) is grayish-yellow medium-grained quartz sandstone. Approximately 5 kg of fresh rock was collected from each sample for zircon separation.

Carbon and oxygen isotope samples: In the carbonate succession of the Quemudongda section, 28 fresh carbonate samples were systematically collected at intervals of 2–5 m. Sampling avoided weathered surfaces, calcite veins, and later tectonic fractures to preserve original sedimentary signatures. In addition, 15 samples were collected from the Que'erchaka section (Bolila Formation)

 doi:10.20944/preprints202605.0178.v1

for regional correlation. All samples were examined by thin-section petrography to confirm lithology and the degree of diagenetic alteration.

Sedimentary facies samples: Typical sedimentary structures, fossils, and special lithological intervals were photographed and sampled in detail. Reef limestones and slump breccias were the main targets, and more than 50 thin sections were prepared for microscopic observation.

3.2. Detrital Zircon U–Pb Dating

Zircon separation and mounting: Clastic rock samples were crushed, panned, and subjected to heavy-liquid and magnetic separation. Zircon grains with euhedral to subhedral shapes, free of visible cracks and inclusions, were handpicked under a binocular microscope. They were mounted together with the reference zircon 91500 in an epoxy resin disk and polished to expose the grain cores.

Cathodoluminescence (CL) imaging: CL imaging was performed at Wuhan SampleSolution Analytical Technology Co., Ltd., using a scanning electron microscope equipped with a CL detector to examine zircon internal structures and to select suitable analytical spots. CL images clearly display oscillatory zoning, indicating a magmatic origin.

LA-ICP-MS U–Pb dating: Zircon U–Pb isotopic analyses were carried out at the same laboratory using laser ablation-inductively coupled plasma-mass spectrometry (LA-ICP-MS). A laser spot size of 32 μm and a repetition rate of 5 Hz were used. The standard zircon 91500 served as the external calibrator for isotopic fractionation, and the standard zircon GJ-1 was used as a quality control monitor. Data reduction was performed with ICP-MS-DataCal software, and common lead correction followed the method of [23]. Age calculation and concordia diagram plotting were conducted using Isoplot/Ex [24].

Age interpretation principle: The youngest group of concordant zircon ages was used to constrain the maximum depositional age of the strata [25]. Because the depositional age of a clastic rock must be younger than the crystallization age of the youngest detrital zircon, this youngest age peak provides a lower limit for the depositional age.

3.3. Carbon and Oxygen Isotope Analysis

Sample preparation: Carbonate samples were cut and cleaned. Under a microscope, areas free of calcite veins and recrystallization were drilled with a micro-drill to obtain approximately 50 mg of powder. Drilling was performed at low speed and low pressure to avoid thermal decomposition.

Isotope measurement: Carbon and oxygen isotope analyses were performed at the State Key Laboratory of Oil and Gas Reservoir Geology and Exploitation, Chengdu University of Technology, using a MultiPrep system coupled to a MAT-253 isotope ratio mass spectrometer. Approximately 200 μg of sample powder was reacted with 100% orthophosphoric acid at 70 °C for 90 min, and the released CO_2 gas was collected and measured. Results are reported relative to the VPDB standard, with analytical precision better than 0.1‰.

Quality control: Internal laboratory standards and the international standard NBS-19 were included in each batch of analyses. Long-term reproducibility is better than ±0.1‰ for $\delta^{13}C$ and ±0.2‰ for $\delta^{18}O$.

Data interpretation: The carbon and oxygen isotopic compositions of carbonates are controlled by multiple factors, including depositional age, paleo-oceanic environment, and diagenesis. This study used multi-section correlation to identify regional age-specific signatures and combined petrographic observations to evaluate the influence of diagenesis [26,27].

4. Results

4.1. Sedimentary Facies Types and Characteristics

The Bolila Formation in the Quemudongda section is dominated by carbonate deposits, with two main sedimentary facies: reef facies and slump breccia facies. These two facies alternate and are

 doi:10.20944/preprints202605.0178.v1

intimately associated, forming a typical steep-rimmed platform-margin depositional association (Figure 2).

4.1.1. Reef Facies

The reef facies is the dominant sedimentary facies of the Bolila Formation, accounting for approximately 75% of the total thickness of the section. Lithologically, it consists mainly of light to dark gray reef limestone and grainstone, with local development of reef dolostone. The biogenic content generally exceeds 50% and can reach up to 80% locally. The reef-building organisms are dominated by hexactinellid and calcareous sponges, with subordinate, sporadic corals and minor sponge-algal binding reefs. The sponges are 1–5 cm in diameter and 2–10 cm high and are well preserved, forming a well-developed sponge framework that provided the material basis for primary porosity in the reservoir.

Diagenetic modification: reef limestones in beds 4, 6, 8–11 and 17 have been significantly dolomitized, forming sponge-reef dolostone. Microscopic observations show that the dolomite crystals are subhedral to euhedral, 0.1–0.5 mm in size, occurring as patches or selectively replacing the biological framework. Vugs 0.5–5 mm in diameter are developed within the rock and show good connectivity, constituting potential reservoir space.

4.1.2. Slump Breccia Facies

The slump breccia facies is symbiotic with the reef facies and directly records platform-margin slope instability. It consists of seven layers, each 1.5–8 m thick, with a total thickness of approximately 32 m, accounting for 9% of the total thickness of the section. Based on lithology, it can be subdivided into limestone breccia (two layers in the lower-middle part) and dolomite breccia (five layers in the upper part). The clasts are angular to subangular, 2 mm to 30 cm in diameter, poorly sorted, and composed mainly of reef limestone clasts; sponge and coral fragments are visible within the clasts. The matrix consists of micrite and sparry calcite; in some layers, the matrix has been completely dolomitized.

Dolomitic breccias exhibit well-developed intra-clast dissolution pores, inter-clast dissolution pores, and dolomite intercrystalline pores. Their pore connectivity is better than that of limestone breccias, and their physical properties are superior, making them the main carrier of high-quality reservoirs in the Bolila Formation.

 doi:10.20944/preprints202605.0178.v1

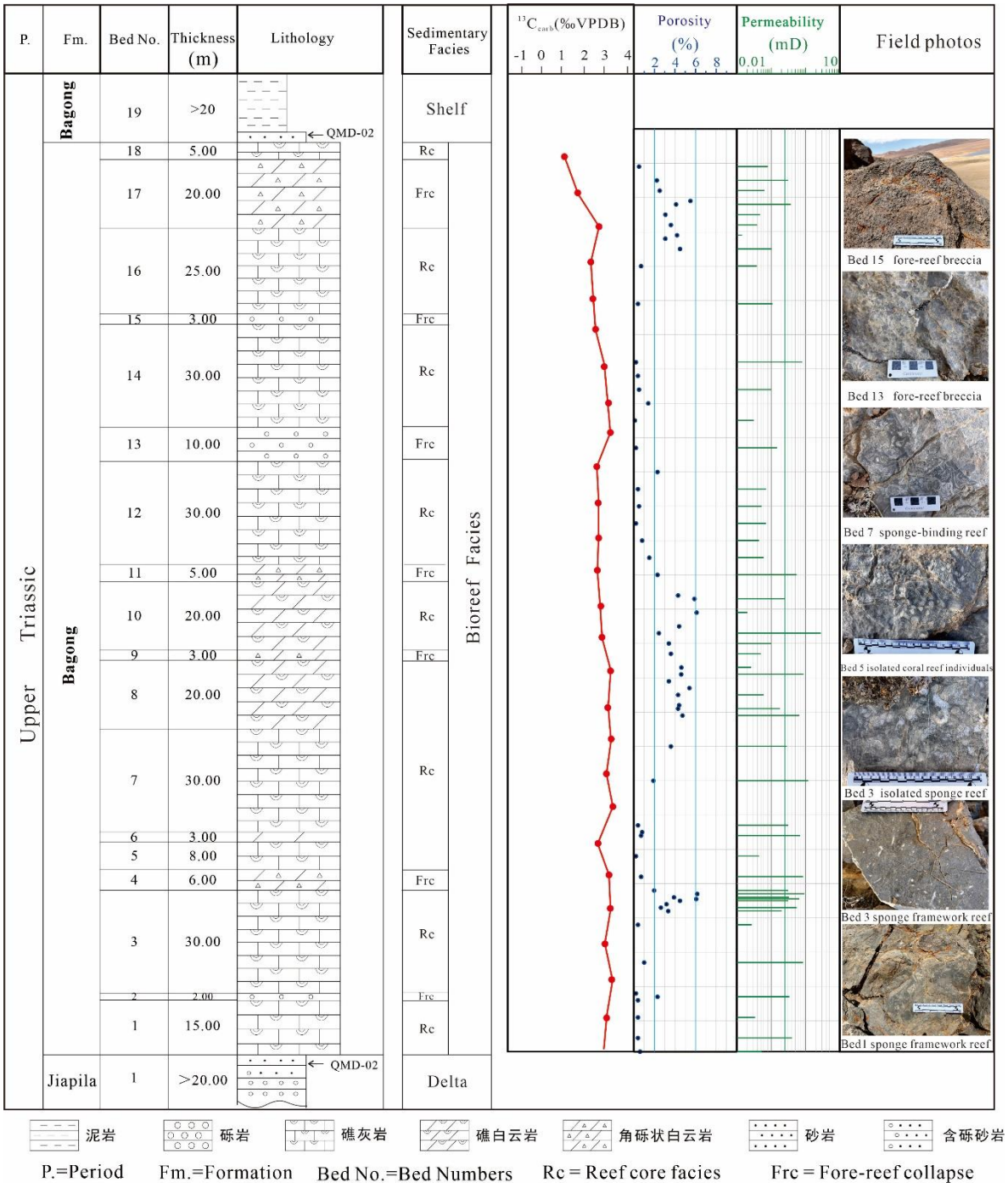

Figure 2. The Quemudongda Comprehensive Stratigraphic Column.

4.2. Detrital Zircon U–Pb Geochronology

To precisely constrain the depositional age of the Bolila Formation, detrital zircon U–Pb dating was performed on clastic rock samples from the base (sample QMD-01) and the top (sample QMD-02) of the section.

Basal sample (QMD-01): The zircons are mostly euhedral to subhedral and show clear oscillatory zoning in CL images. Except for three grains, their Th/U ratios range from 0.22 to 1.59, indicating a magmatic origin. A total of 86 zircon grains were analyzed, yielding 76 concordant ages (concordance >90%). The age spectrum (Figure 3a) shows two main age populations at 300–400 Ma (peak ~350 Ma) and 600–800 Ma (peak ~700 Ma), with minor peaks at 1800–2000 Ma and >2500 Ma. The weighted mean age of the youngest zircon group is 242.6 ± 3.3 Ma (n=6, MSWD=1.3), and the youngest single-

 doi:10.20944/preprints202605.0178.v1

grain age is 235.7 ± 2.5 Ma (Figure 3b). This youngest single-grain age constrains the maximum depositional age of the Bolila Formation to no older than the early Carnian (Late Triassic).

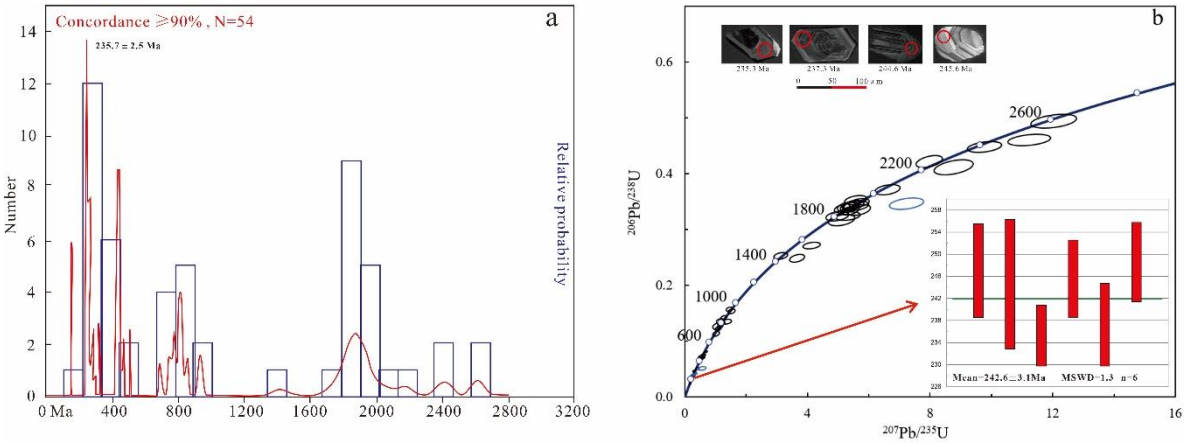

Figure 3. U–Pb Dating Results of Detrital Zircons from Sample QMD-01.

Top sample (QMD-02): The zircon characteristics are similar to those of the basal sample, with Th/U ratios ranging from 0.14 to 2.57 (except for four grains). A total of 92 zircon grains were analyzed, yielding 83 concordant ages. The age spectrum (Figure 4a) shows age populations mainly at 300–500 Ma (peak ~430 Ma) and 1800–2000 Ma. The weighted mean age of the youngest zircon group is 225.7 ± 3.4 Ma (n=5, MSWD=1.9) (Figure 4b), which constrains the minimum depositional age of the top of the Bolila Formation to the Norian (Late Triassic).

Integrating the two dating results, the depositional age of the Bolila Formation is constrained to 225.7–235.7 Ma, corresponding to the Carnian–Norian stages of the Late Triassic. This provides a high-precision chronostratigraphic framework for subsequent sedimentary evolution analysis and regional stratigraphic correlation.

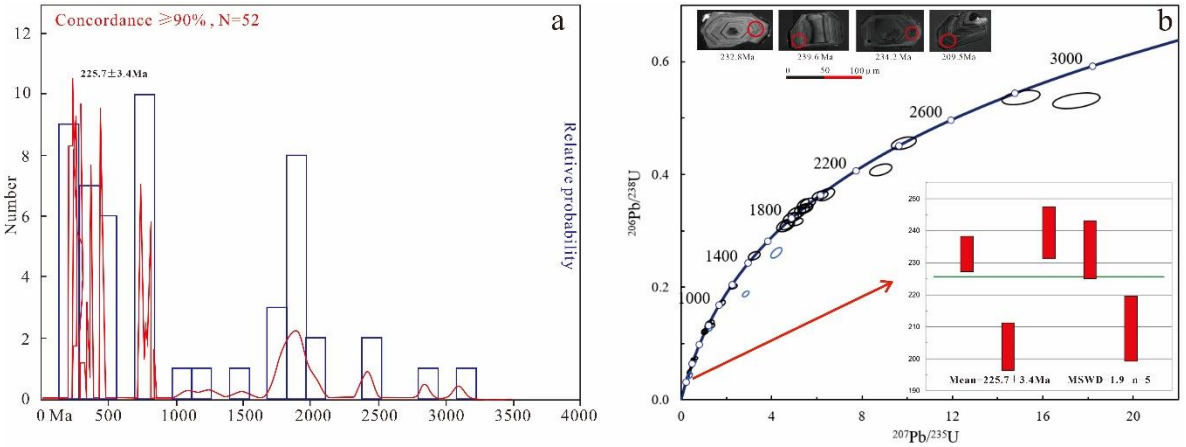

Figure 4. U–Pb Dating Results of Detrital Zircons from Sample QMD-02.

4.3. Carbon and Oxygen Isotope Characteristics

To reconstruct the paleo-marine environment during deposition of the Bolila Formation, 28 carbonate samples from the Quemudongda section and 15 from the Que'erchaka section were analyzed for carbon and oxygen isotopes. Samples showing obvious recrystallization or calcite veins were excluded based on thin-section inspection prior to analysis.

Quemudongda section: $\delta^{13}C$ ranges from +1.3‰ to +4.0‰, with a mean of +3.2‰ (median +3.1‰, standard deviation 0.6‰), indicating a stable positive shift. $\delta^{18}O$ ranges from –14.3‰ to –

 doi:10.20944/preprints202605.0178.v1

7.0‰, with a mean of –11.1‰ (median –11.3‰, standard deviation 1.5‰), showing a strong negative shift. There is no significant correlation between $\delta^{13}C$ and $\delta^{18}O$ (R^2 = –0.17, Figure 5a), suggesting limited diagenetic alteration [27].

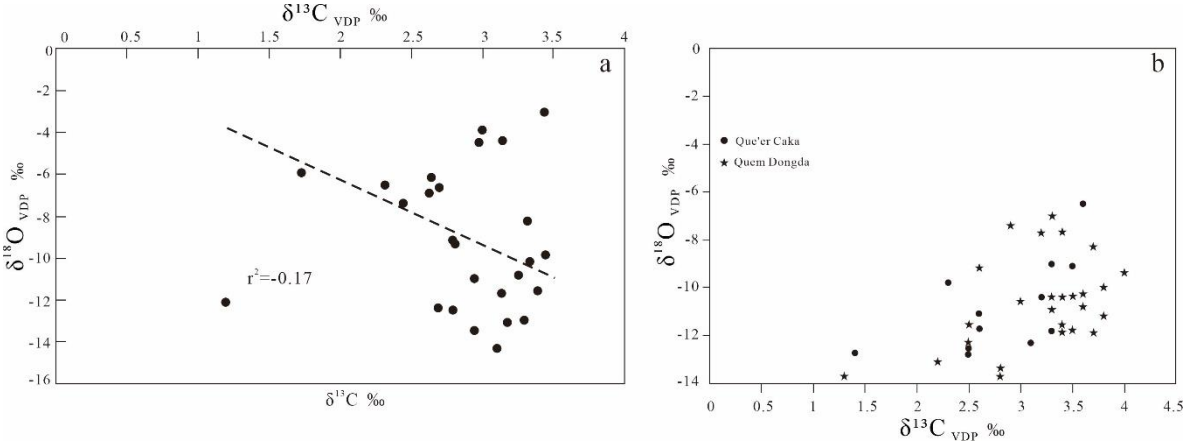

Figure 5. Carbon and oxygen isotope characteristic diagram of the Bolila Formation.

Que'erchaka section: $\delta^{13}C$ averages +2.7‰, and $\delta^{18}O$ averages –11.5‰. The carbon-oxygen isotopic distributions of the two sections show similar characteristics (Figure 5b), indicating that they were deposited in the same paleo-ocean environment and reflecting regional uniformity in paleo-ocean chemical conditions in the central Qiangtang Basin during the Carnian–Norian.

The carbonates of the Bolila Formation are characterized by a "high positive $\delta^{13}C$ and strong negative $\delta^{18}O$" isotopic fingerprint, which can serve as an important geochemical identifier for this formation.

4.4. Reservoir Properties and Pore Types

The reservoir characteristics of the Bolila Formation are described based on petrological, cast thin-section, and conventional physical property analyses.

4.4.1. Reservoir Rock Types and Distribution

The reservoir rocks of the Bolila Formation are mainly carbonates, including reef dolostone, breccia dolostone, reef limestone, breccia limestone, and grainstone. Reef dolostone and breccia dolostone are the main reservoir rock types, with a cumulative potential reservoir thickness of about 265 m. Microscopic characteristics are as follows:

Dolostone: medium to coarse crystalline texture, well-developed intercrystalline pores; locally exhibits selective replacement of biological frameworks (Figure 6A).

Breccia limestone: clast size >2 mm, with dissolution fissures along clast margins; matrix is mainly micrite (Figure 6B).

Grainstone: grain size 0.3–2 mm, cemented by sparry calcite; primary pores are mostly filled (Figure 6C).

Bioclastic limestone: contains bivalve and gastropod fragments; cavities are filled with micrite, resulting in poorly developed reservoir space (Figure 6D).

 doi:10.20944/preprints202605.0178.v1

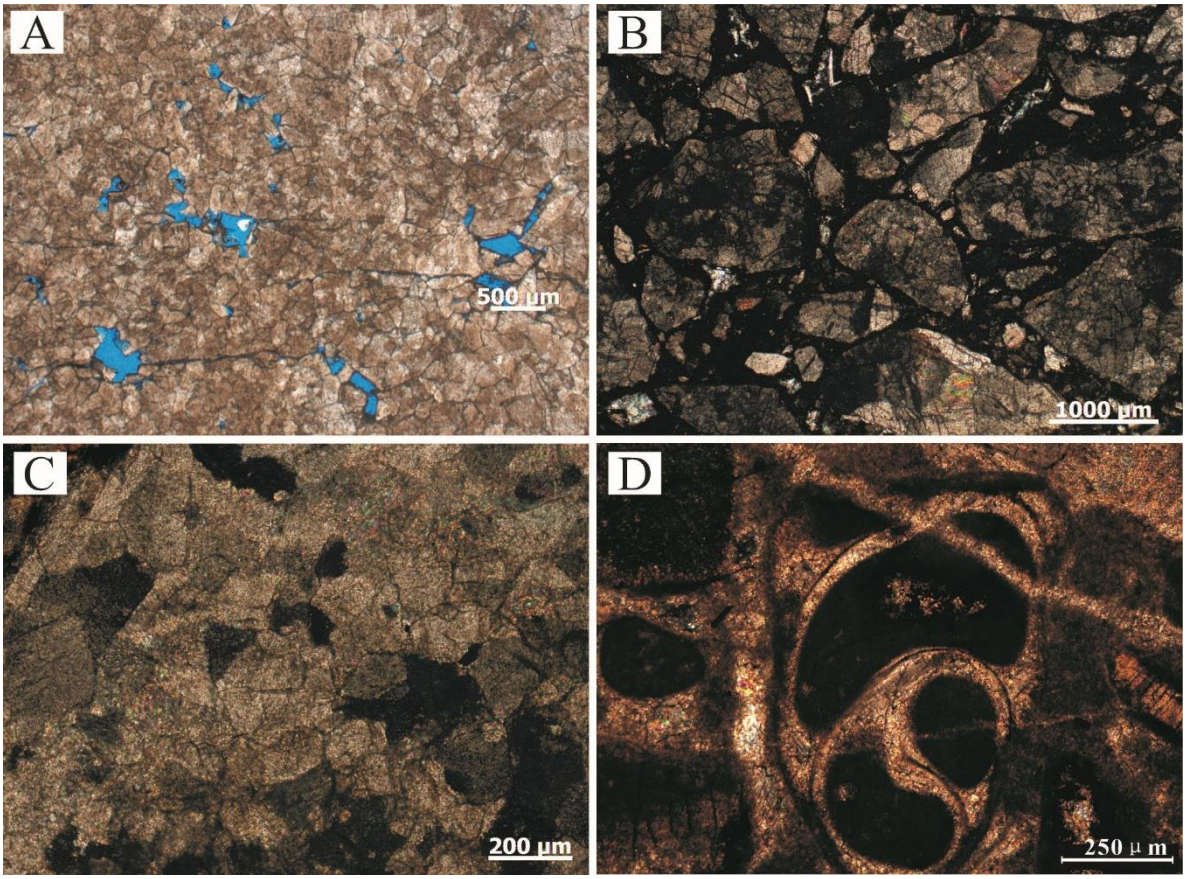

Figure 6. Microscopic characteristics of reservoir rock types of the Bolila Formation. (A) Dolostone; (B) Breccia limestone; (C) Grainstone; (D) Bioclastic limestone.

4.4.2. Pore Types and Characteristics

Six main pore types are identified from cast thin sections (Figure 7). Among them, intergranular dissolution pores, intercrystalline pores, and fracture-related dissolution pores contribute most to reservoir quality:

Intergranular dissolution pores: formed by dissolution of intergranular cements, irregular shape, pore size 0.01–1.6 mm, good connectivity; one of the main effective pore types.

Intragranular dissolution pores: formed within grains, pore size <0.01 mm, poor connectivity.

Intercrystalline pores and intercrystalline dissolution pores: developed in dolostone, consist of pores between dolomite crystals and their dissolution-enlarged equivalents; angular to polygonal, pore size 0.02–0.1 mm, moderate to good connectivity.

Fracture-related dissolution pores: formed by dissolution along tectonic fractures, variable pore size, good connectivity, can significantly improve permeability.

Stylolites: zigzag or wavy, 0.01–0.25 mm wide, often filled with organic matter or bitumen; mostly ineffective pores.

 doi:10.20944/preprints202605.0178.v1

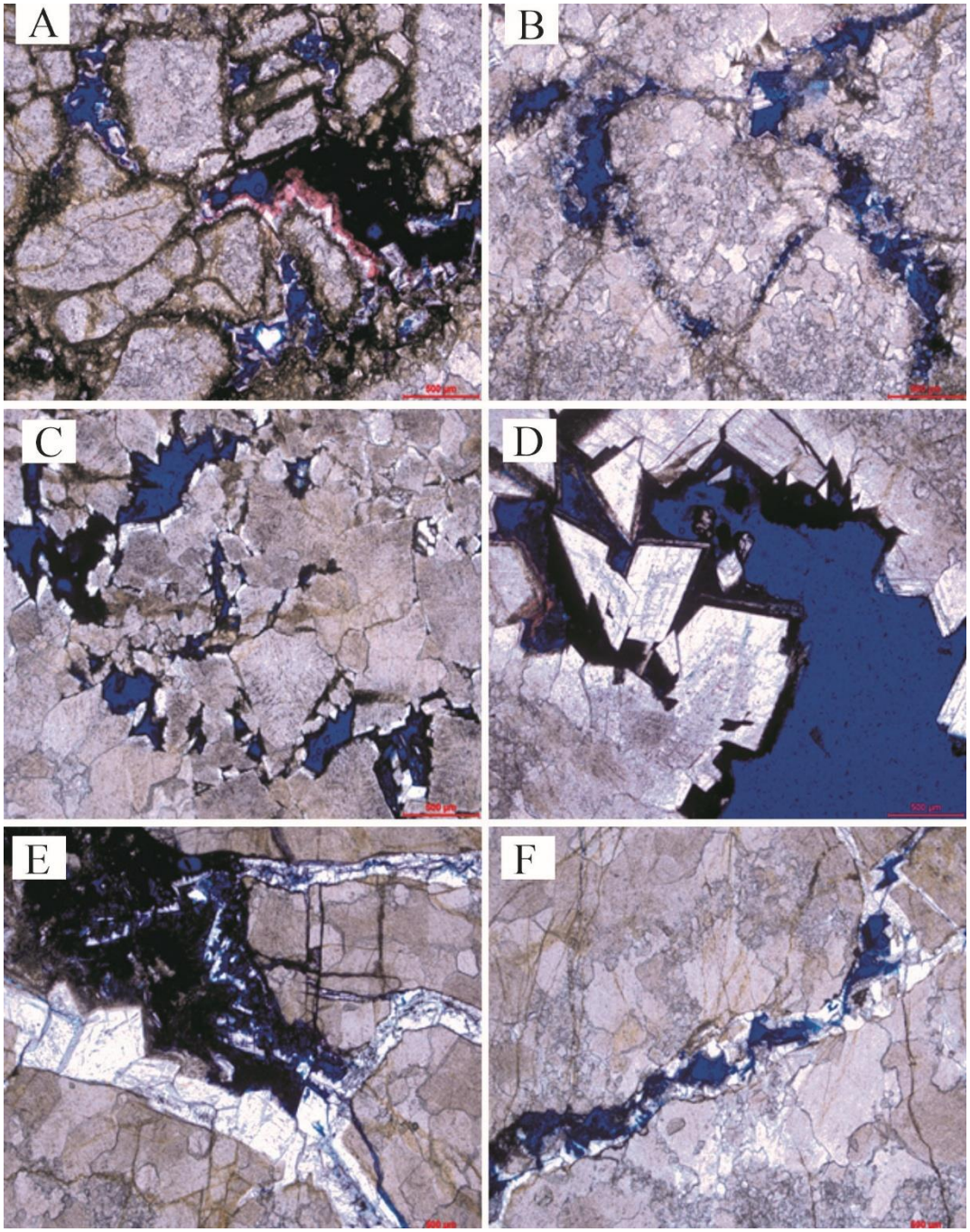

Figure 7. Microscopic characteristics of pore types of the Bolila Formation. (A) Intergranular dissolved pores; (B) Stylolites; (C) Intragranular and intergranular dissolved pores; (D) Intercrystalline pores and intercrystalline dissolved pores; (E) Intra-fracture dissolved pores; (F) Pressure solution fractures. Cast thin section; blue represents cast resin, plane-polarized light.

4.4.3. Porosity and Permeability Characteristics

Conventional physical property tests were performed on 22 representative reservoir samples:

Porosity: ranges from 0.8% to 7.2%, with an average of 2.8%; within this range, 2–4% accounts for 47.4%, <2% for 31.6%, and >4% for 21.0%, indicating generally low porosity (Figure 8A).

Permeability: ranges from 0.001 to 8.5 mD, spanning four orders of magnitude; within this range, <0.25 mD accounts for 42.1%, 0.25–1 mD for 26.3%, and >1 mD for 31.6%, indicating overall ultra-low permeability with locally relatively high-permeability intervals (Figure 8B).

 doi:10.20944/preprints202605.0178.v1

Physical properties vary significantly with lithology: breccia dolostone (bed 4, n=8) has an average porosity of 3.71% and an average permeability of 2.412 mD, representing the best reservoir quality; reef dolostone (beds 10 and 17, n=10) has average porosity of 2.01–3.31% and average permeability of 0.134–1.019 mD. The correlation between porosity and permeability is very weak (R^2 = 0.19) (Figure 9), indicating that the reservoir is a fracture-pore dual-media reservoir, with permeability mainly controlled by fractures and dissolution vugs rather than by matrix pores.

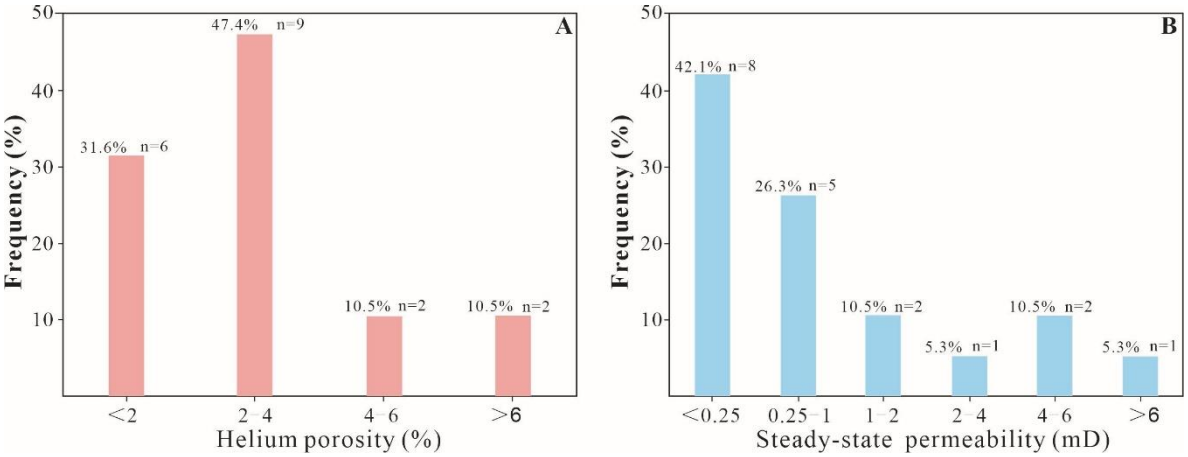

Figure 8. Histogram of porosity and permeability of the Bolila Formation.

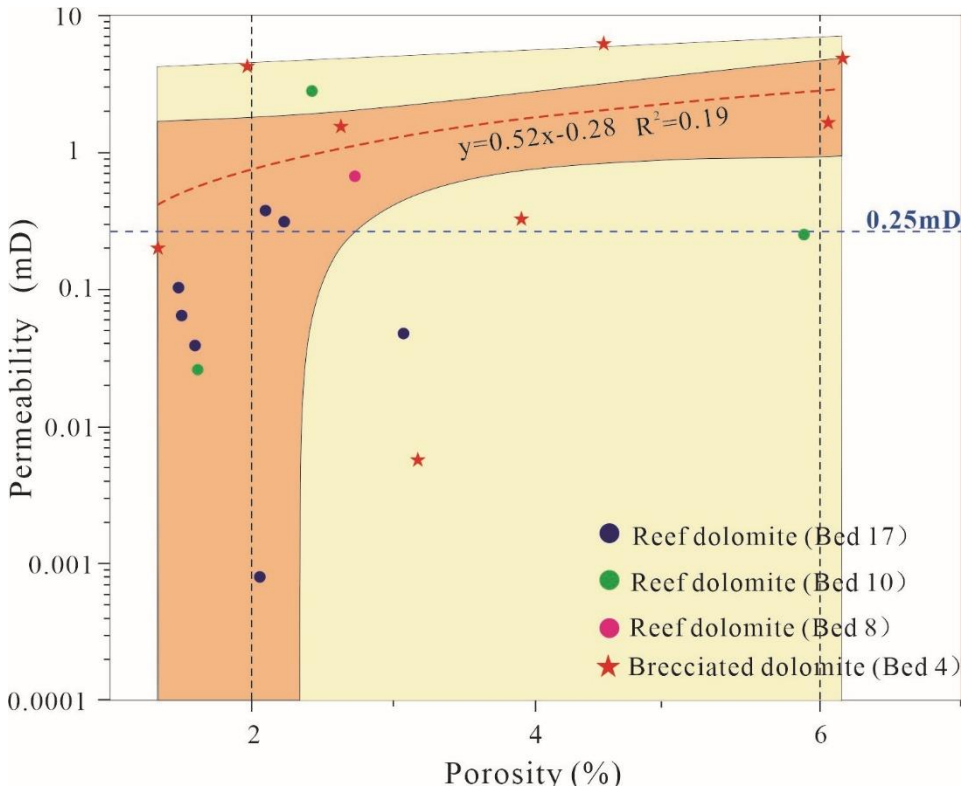

Figure 9. Porosity–permeability correlation diagram of the Bolila Formation.

5. Discussion

5.1. Stratigraphic Age Constraints and Regional Correlation

Integrating detrital zircon U–Pb geochronology, carbon-oxygen isotopes, and regional biostratigraphic data, the depositional age of the Bolila Formation is refined, correcting previous

 doi:10.20944/preprints202605.0178.v1

stratigraphic miscorrelations and establishing a temporal framework for sedimentary evolution analysis.

5.1.1. Zircon U–Pb Geochronological Constraints

The youngest single-grain age of 235.7 ± 2.5 Ma from the basal sample and the youngest weighted mean age of 225.7 ± 3.4 Ma from the top sample constrain the depositional age of the Bolila Formation in the Quemudongda section to 225.7–235.7 Ma, corresponding to the Carnian–Norian stages of the Late Triassic [28].

It is noteworthy that the weighted mean age of the youngest zircon group from the basal sample is 242.6 ± 3.3 Ma (n=6), slightly older than the traditional base of the Upper Triassic (ca. 237 Ma). This age peak likely records a late Ladinian (Middle Triassic) magmatic event in the source area (ca. 242 Ma); these zircons were eroded and deposited into the basal Bolila Formation and do not represent the depositional age itself. The youngest single-grain age of 235.7 ± 2.5 Ma (concordance >95%, Th/U = 0.68) provides a more reliable estimate of the maximum depositional age. Such a discrepancy is common in detrital zircon geochronology: the youngest peak age often reflects multiple magmatic episodes in the source area and is thus older, whereas the youngest single-grain age more faithfully records the depositional age [25,29].

Regionally, the lower part of the Bolila Formation in the Quemo Co area yields Carnian bivalves Halobia convexa and H. yunnanensis [30], corroborating the 235.7 Ma age obtained here. Therefore, the Bolila Formation began to accumulate in the early Carnian (Late Triassic), not in the late Middle Triassic.

5.1.2. Carbon and Oxygen Isotope Evidence

(1) Assessment of diagenetic alteration

Carbon and oxygen isotopic compositions of carbonates are susceptible to post-depositional diagenesis. To assess data reliability, we examined thin sections: all analyzed samples lack significant recrystallization and calcite veins; moreover, $\delta^{13}C$ and $\delta^{18}O$ show no significant correlation ($R^2 = -0.17$), indicating limited diagenetic overprinting [27]. Thus, the isotopic data are suitable for paleoenvironmental reconstruction and stratigraphic correlation.

(2) Paleoenvironmental significance of positive $\delta^{13}C$ shifts

The mean $\delta^{13}C$ value of the Bolila Formation is +3.2‰, significantly higher than the background of normal marine carbonates (ca. 0‰ to +2‰), consistent with the global Late Triassic Carnian–Norian positive $\delta^{13}C$ excursion [31,32]. This positive shift is interpreted as a combined response to increased terrestrial nutrient input, enhanced marine primary productivity, and accelerated organic carbon burial during the Carnian Pluvial Event (CPE) [33–35]. The stable positive $\delta^{13}C$ values (71% of samples in the range +2.8‰ to +3.5‰) indicate that the marine carbon cycle remained relatively stable during deposition of the Bolila Formation, sustaining high productivity.

(3) Paleoclimatic implications of negative $\delta^{18}O$ shifts

The strongly negative $\delta^{18}O$ values (mean –11.1‰) are far lower than the typical background of normal marine limestones (–5‰ to 0‰), reflecting a combination of two possible mechanisms:

① High-temperature effect: Using the $\delta^{18}O$-temperature relationship [36] and assuming a seawater $\delta^{18}O$ of –1‰ (to account for fresh-water input), the calculated paleo-seawater temperature is approximately 30–35 °C, which is significantly higher than the modern tropical average (~25 °C). This high-temperature regime is consistent with the global hyperthermal climate during the Carnian–Norian [32,37].

② Fresh-water input effect: During the CPE, global precipitation increased dramatically, and large volumes of ^{16}O-enriched fresh water entered the ocean, lowering seawater $\delta^{18}O$ [33–35]. Regionally, the widespread occurrence of deltaic coal-bearing clastic rocks in Carnian strata on the northern margin of the Qiangtang Basin [13,14] indicates significantly enhanced terrigenous input and a non-negligible influence of fresh water on the shallow-marine environment. Therefore, the

 doi:10.20944/preprints202605.0178.v1

strongly negative $\delta^{18}O$ values in the study area most likely reflect the combined effects of high temperature and fresh-water input.

(4) Global correlation and stratigraphic discrimination

The positive $\delta^{13}C$ excursion in the Quemudongda section can be well correlated with Carnian records from the Dolomites (Italy) [33], the Lunz section (Austria) [38], and the Nanpanjiang Basin (South China) [35], indicating the global nature of this carbon-isotope event.

Notably, the "high-positive $\delta^{13}C$ and strongly negative $\delta^{18}O$" signature of the Bolila Formation contrasts sharply with that of the Middle Jurassic Buqu Formation ($\delta^{13}C$ +1‰ to +3‰, $\delta^{18}O$ –8‰ to –3‰) [39,40], providing an effective geochemical tool for distinguishing these two key carbonate units in the Qiangtang Basin and for regional stratigraphic calibration.

In summary, the carbon and oxygen isotope characteristics of the Bolila Formation record a stable shallow-marine environment under a global warm and humid climate during the Carnian–Norian, supporting the interpretation that the study area was a high-energy platform-margin facies belt.

5.1.3. Regional Biostratigraphic Verification

Regional biostratigraphic data show that the underlying Jiapila Formation contains typical brachiopod fossils, and the Bolila Formation itself contains corals and bivalves (e.g., Halobia spp.) [21], all of which are typical Carnian–Norian (Late Triassic) elements, consistent with the detrital zircon U–Pb ages. Collectively, the evidence confirms that the stratigraphic succession in the Quemudongda section belongs to the Upper Triassic Bolila Formation, correcting the erroneous Jurassic assignment on the 1:250,000 geological map and providing a reliable basis for regional stratigraphic correlation.

5.2. Sedimentary Evolution Characteristics and Model of the Bolila Formation

Based on sedimentary facies, carbon-oxygen isotopes, and geochronology, combined with the regional tectonic setting, the sedimentary evolution of the Bolila Formation (Carnian–Norian, Late Triassic) is systematically reconstructed, and the sedimentary facies associations and regional paleogeographic implications are clarified.

5.2.1. Sedimentary Facies Associations and Depositional Environments

The Quemudongda section exhibits a complete sedimentary succession of "reef facies – slump breccia facies – lime mudstone/mudstone facies". The close association of reef and slump breccia facies is a hallmark of steep-rimmed carbonate platform margins [41,42].

Reef facies: Developed on the high-energy platform margin, where strong wave action, ample sunlight, and good nutrient supply offered an ideal niche for reef-building sponges. The reef is dominated by hexactinellid and calcareous sponges, forming a wave-resistant sponge framework. Corals occur as sporadic patches, reflecting local environmental fluctuations; binding reefs are minor and have limited influence on the overall depositional pattern. The vertical stacking of the reef facies indicates episodic reef growth, closely linked to sea-level changes and sedimentation rates.

Slump breccia facies: Closely associated with the reef facies, this facies consists of seven layers, each 1.5–8 m thick, with a total thickness of about 32 m. The clasts are angular to subangular, 2 mm to 30 cm in diameter, very poorly sorted, and composed mainly of reef limestone clasts containing sponge and coral fragments. The matrix is micrite and sparry calcite; in some layers the matrix is completely dolomitized. These features indicate a proximal, rapidly deposited product with short transport distances and high accumulation rates. The seven slump breccia layers record multiple episodic slope-failure events, which may have been triggered by: (1) storm-induced gravity flows; (2) seismic shocks from syn-sedimentary faulting; or (3) oversteepening of the slope due to excessive reef progradation [43,44].

 doi:10.20944/preprints202605.0178.v1

Regional lateral differentiation: Based on 1:250,000 regional geological survey data and our new field measurements, the Bolila Formation exhibits significant lateral lithological zonation in the study area and adjacent regions, reflecting the control of paleogeography on sedimentary facies:

Eastern and western platform-margin belts (e.g., Quemudongda, Juhuashan): dominated by reef limestone and dolostone. Reef limestone has a cumulative thickness of 80–120 m and contains coral, stromatoporoid, and algal reef fossils. Dolostone is mostly medium- to fine-crystalline, locally with patchy structures, indicating a high-energy, salinity-fluctuating shallow platform-margin environment.

Central Que'erchaka area: dominated by alternating grainstone and dolostone. Grainstone is 60–90 m thick, with skeletal, oolitic, and bioclast grains accounting for 65–80%, well sorted and rounded, with cross-bedding, parallel bedding, and tidal bedding, indicating a high-energy shallow-platform shoal environment.

Jiang'aidarina and Juhuashan areas: dominated by shallow-shelf micritic limestone and lime mudstone, with a total thickness of 200–250 m. The rocks are fine-grained (grain size <0.01 mm) and dense, with horizontal bedding and bioturbation structures; organic matter content is 0.8–1.5%, with occasional planktonic foraminifera and radiolaria, indicating a low-energy, stable shelf environment.

This lateral differentiation shows that the paleogeography during deposition of the Bolila Formation was characterized by a complete "inner platform – platform margin – platform-margin slope – shelf" facies tract, providing spatial constraints for establishing the sedimentary evolution model.

5.2.2. Sedimentary Evolution Model

During the Carnian–Norian, the Qiangtang block was located at a low latitude on the northern margin of the Paleo-Tethys Ocean, with a warm and humid climate [9,13]. Caused by regional transgression associated with the expansion of the Bangong Co–Nujiang oceanic basin, a broad carbonate platform developed in the North Qiangtang Depression. The Quemudongda section is situated on the platform-margin slope break, forming a paleogeographic pattern of "shallow-water inner platform to the south, and slope-basin to the north". Based on the vertical facies succession, geochronology, and sea-level curves, the sedimentary evolution of the Bolila Formation is divided into three stages:

Stage I: Early Carnian (235.7–230 Ma) – Early transgression, reef initiation

Sea level was relatively low, and deposition began on the platform margin. The water was shallow, with moderate wave action. Sponges and other reef builders started to form small patch reefs on the high-energy platform margin; the reefs were thin and limited in extent. The slope was gentle, and slumping events were few. This stage is characterized by reef limestone and fore-reef grainstone, with primary pores developed, but a large-scale reef framework had not yet formed.

Stage II: Late Carnian – early Norian (230–228 Ma) – Peak transgression, reef flourishing

Sea level rose rapidly to its highest stand. The platform margin had suitable water depths (ca. 20–50 m) and ample nutrient supply, allowing the sponge reefs to enter a phase of rapid growth. The reefs grew upward and seaward, forming a thick framework, and the fore-reef slope became progressively steeper. As the slope steepened, periodic failure occurred under gravity, storms, or syn-sedimentary faulting, producing multiple slump breccia layers (seven in total). This stage represents the main phase of reef construction in the Bolila Formation and the period of most frequent slope failures.

Stage III: Late Norian (228–225.7 Ma) – Regression, reef decline and dolomitization

Sea level gradually fell, the water became shallower, reef growth slowed, and slumping events decreased. Some reefs were exposed or shallowly buried and underwent penecontemporaneous to shallow-burial dolomitization, forming reef dolostone and breccia dolostone. Primary pores were partly modified, intercrystalline pores developed, laying a foundation for later reservoir formation. At the end of this stage, regression continued, and the carbonate platform was replaced by clastic

 doi:10.20944/preprints202605.0178.v1

deposits (Bagong Formation), marking the termination of carbonate sedimentation in the Bolila Formation.

This evolution is well correlated with global Carnian sea-level curves [45,46] and the climatic fluctuations of the CPE. The peak transgression of Stage II coincides with the main phase of the CPE (~232–228 Ma), when increased global rainfall and enhanced terrigenous input may have promoted nutrient supply and reef flourishing [33,35].

5.2.3. Regional Paleogeographic Implications

The recognition of the platform-margin facies belt in the Quemudongda section has important implications for reconstructing the Late Triassic paleogeography of the Qiangtang Basin.

Redefinition of the platform-margin position: The 1:250,000 geological map placed the area around the Quemudongda section within a Jurassic stable inner-platform facies, and accordingly the Late Triassic paleogeographic map assigned this area to an inner-platform setting. This study demonstrates that this area is actually a Late Triassic platform-margin facies belt, implying that the platform margin in the South Qiangtang Depression should be shifted 20–30 km northward. The revised paleogeographic framework is "inner platform (Que'erchaka) – platform margin (Quemudongda) – platform-margin slope – shelf (Jiang'aidarina, Juhuashan)".

Spatial configuration of platform-basin facies belts: Combined with regional geological data [19,20], the South Qiangtang Depression exhibits a clear platform–slope–basin differentiation during the Late Triassic: the inner platform (Que'erchaka) contains open-platform limestones; the platform margin (Quemudongda) features reef-slump breccia associations; and to the north, this passes into slope-basin dark mudstones and siliceous rocks. This paleogeographic framework provides a valuable basis for facies analysis and hydrocarbon exploration deployment.

Recognition of the Central Uplift as a source area: The abundant Paleozoic detrital zircon ages (300–500 Ma, 1800–2000 Ma) in the basal Bolila Formation indicate a provenance mainly from the Central Uplift, suggesting that the Central Uplift was already an important source area during the Late Triassic [14,47]. This supports the view that the Central Uplift had emerged as positive relief in the early Late Triassic, supplying clastic material to the basins on both sides.

Comparison with global typical platform margins: The reef-slump breccia association in the Quemudongda section is comparable to that in the Upper Triassic Dachstein reefs of the Alps [42] and the Permian Guadalupe Mountains reef complex of North America [48], indicating that the sedimentary dynamics along the Late Triassic platform margin of the Qiangtang Basin were similar to those of other classic steep-rimmed carbonate platforms, further supporting the interpretation of a low-latitude, warm-water setting for the Qiangtang block at that time.

In summary, the sedimentary evolution of the Bolila Formation was controlled by regional sea-level changes and tectonic subsidence, resulting in a complete "reef construction – slope slumping – dolomitic alteration" depositional-diagenetic sequence that provided favourable material and space for subsequent reservoir development.

5.3. Reservoir-Forming Effects and Controlling Factors

Combining reservoir petrology, pore types, and diagenetic characteristics, the reservoir-forming process, main controlling factors, and distribution of high-quality reservoirs in the Bolila Formation are analysed, and a "sedimentation-diagenesis-tectonics" triple-play reservoir-forming model is established.

5.3.1. Impact of Dolomitization on Reservoir Quality

Dolostones in the Bolila Formation are mainly finely to medium-crystalline and display xenotopic (anhedral) crystal contacts, rather than the euhedral–subhedral, sucrosic texture commonly associated with classic dolomitization. Microscopic observations show irregular, zigzag to stylolitic crystal boundaries that have strongly compressed or even eliminated primary intercrystalline pores.

 doi:10.20944/preprints202605.0178.v1

This feature is the direct cause of the generally low matrix porosity (average <4%) in these dolostones, contrasting sharply with the volume contraction (ca. 12–13%) [49,50] predicted by the classical "mole-per-mole" replacement model, which would produce euhedral–subhedral intercrystalline pores.

Dolomitization makes three constructive contributions to reservoir quality: (1) Increased brittleness – dolostone is mechanically more brittle than limestone, more prone to fracturing under tectonic stress, producing transgranular microfractures and grain-boundary fractures that serve as fluid pathways [51]; (2) Selective dissolution – dolomite crystal boundaries and interiors are susceptible to dissolution, generating intercrystalline dissolution pores that effectively enhance reservoir space [52]; (3) Residual volume-shrinkage pores – although most intercrystalline pores were compressed by recrystallization, a small number of residual pores remain, providing a basis for later dissolution.

Nevertheless, the dolostones in the study area are generally tight, due to two factors: (1) High-temperature recrystallization – the Bolila Formation was deposited during the global hot-climate interval of the Carnian–Norian [32,37]; elevated paleotemperatures (burial stage up to 60–100 °C) promoted recrystallization of dolomite from euhedral–subhedral to xenotopic textures, drastically reducing intercrystalline porosity [53,54]; (2) Lack of later dissolution – the dolostones did not experience extensive meteoric-water leaching or organic-acid dissolution during burial, so pores could not be enlarged or connected [55]. This feature is similar to the origin of Middle Jurassic Buqu Formation dolostones in the South Qiangtang Depression, which were also affected by burial high-temperature recrystallization [40].

5.3.2. Contribution of Fractures to Reservoir Quality

The porosity-permeability correlation in the Bolila Formation reservoirs is very weak (R^2 = –0.17), and some low-porosity samples exhibit relatively high permeability (e.g., breccia dolostone reaching 6.31 mD), indicating that microfracture networks are the primary control on permeability [56]. Three main types of fractures are identified:

Transgranular microfractures: cut through dolomite crystals, generally 0.005–0.02 mm wide, laterally extensive, good connectivity.

Grain-boundary fractures: developed along grain margins, often associated with dissolution, forming fracture-related dissolution pores.

Opened stylolites: some pressure-dissolution stylolites were opened by later tectonic activity, with apertures of 0.01–0.25 mm, can act as fluid conduits.

These microfractures contribute little to pore volume (typically <1%), but as preferred fluid pathways they can dramatically increase permeability (following the "cubic law"), creating a "low porosity – relatively high permeability" anomalous property combination. Fracture development is related to the following tectonic events: (1) the mildly extensional to structurally relaxed setting during the Late Triassic–Early Jurassic, which generated extensional microfractures; (2) polyphase tectonic compression during the Yanshanian and Himalayan orogenies, which opened earlier fractures and created new shear fractures [57,58]. Therefore, fracture-development zones are critical for forming high-quality reservoirs.

5.3.3. Integrated Analysis of Controlling Factors

Reservoir development in the Bolila Formation is controlled by the interplay of sedimentation, diagenesis, and tectonics, summarized as "sedimentary facies control material foundation, diagenesis controls pore evolution, tectonics controls permeability".

(1) Sedimentary facies – material foundation for reservoir formation

The high-energy platform-margin facies belt (reef, slump breccia, and shoal facies) is the most favourable for high-quality reservoirs. These facies have the following characteristics: ① rock types dominated by grainstones, reef limestones, and breccias, with grain-supported fabrics that resist compaction, and well-developed primary intergranular and intraskeletal pores [59]; ② high depositional energy resulting in low micrite content, favouring preservation of primary pores; ③

 doi:10.20944/preprints202605.0178.v1

high-energy settings facilitate circulation of later diagenetic fluids and dolomitization/dissolution. In contrast, low-energy inner-platform micritic limestones have scarce primary pores and generally poor physical properties (porosity mostly <1.5%, permeability <0.01 mD) and are unlikely to form effective reservoirs.

(2) Diagenesis – key control on pore evolution

The interplay of constructive and destructive diagenetic processes determines final reservoir properties:

Constructive diagenesis: ① dolomitization – generates intercrystalline pores and increases brittleness; ② dissolution – selective dissolution along intergranular pores, intercrystalline pores, and fractures produces intergranular dissolution pores, intercrystalline dissolution pores, and fracture-related dissolution pores, effectively enlarging reservoir space; ③ fracturing – creates microfracture networks that significantly enhance permeability.

Destructive diagenesis: ① xenotopic recrystallization – severely compresses intercrystalline pores, densifying the matrix; ② calcite cementation – fills primary and dissolution pores, reducing porosity and permeability; ③ mechanical compaction and pressure dissolution – cause grains to contact along lines or become interlocked, eliminating primary pores.

(3) Tectonics – engine for permeability enhancement

During the Late Triassic, the North Qiangtang Basin was in a post-collisional, mildly extensional to structurally relaxed stage [5]. This stable tectonic setting provided accommodation space for development of a thick, widespread carbonate platform and favourable conditions for dolomitization. Moreover, episodic tectonic activity had a dual effect: ① it triggered platform-margin slope failures, forming slump breccias whose inter-clast pores and intra-clast fractures provided initial reservoir space; ② it produced syn-depositional and later tectonic fractures that became preferred fluid pathways. Polyphase Yanshanian and Himalayan compression further opened and extended earlier fractures, enhancing the fracture network.

High-quality reservoir development: Reservoirs of the Bolila Formation are generally low-porosity, ultra-low-permeability fracture-pore type. High-quality reservoirs (Class I, permeability >0.25 mD) require the following conditions: ① location in the platform-margin facies belt (reef, slump breccia, shoal); ② dolomitization and dissolution, developing intercrystalline and dissolution pores; ③ location in a fracture-development zone where microfracture networks connect isolated pores. All three conditions are necessary; the breccia dolostone–fracture overlap zone is the core area for high-quality reservoir development.

In summary, the reservoir-forming effect of the Bolila Formation can be summarized as: the high-energy platform-margin facies provided primary pores and a compaction-resistant rock framework; dolomitization and dissolution modified and enlarged the pore space; tectonic fractures enhanced permeability; their combination produced a “low porosity – relatively high permeability” fracture-pore reservoir. This understanding provides a theoretical basis for carbonate reservoir evaluation and hydrocarbon exploration deployment in the Qiangtang Basin.

5.4. Tectono-Sedimentary Evolution and Hydrocarbon Exploration Significance

Integrating regional tectonic setting, sedimentary evolution, and reservoir-forming effects, the hydrocarbon exploration value of the Bolila Formation is clarified, achieving a logical closure from “sedimentary evolution – reservoir formation – hydrocarbon exploration”.

5.4.1. Tectonic Control on Sedimentation and Reservoir Formation

Detrital zircon age spectra provide important constraints on the tectonic setting during deposition of the Bolila Formation. Both the basal and top samples from the Quemudongda section show multi-peak age spectra with peaks mainly at 300–500 Ma (Early Paleozoic), 600–800 Ma (Neoproterozoic), and 1800–2000 Ma (Paleoproterozoic), lacking the unimodal arc-derived zircon ages of the Early–Middle Triassic (250–240 Ma). This contrasts sharply with the unimodal arc-derived age spectra commonly observed in the Early–Middle Triassic foreland basin stage of the North

 doi:10.20944/preprints202605.0178.v1

Qiangtang area [60], indicating that the Paleo-Tethys Ocean had already closed before deposition of the Bolila Formation, and the North Qiangtang area was no longer affected by arc magmatism related to subduction of the Hoh Xil–Jinshajiang Ocean [22,34].

During the Carnian–Norian, the North Qiangtang Basin was in a post-collisional mildly extensional to structurally relaxed stage [5]. This tectonic background had multiple effects on the sedimentation-reservoir process of the Bolila Formation:

Stable development of the carbonate platform: Mild extension allowed stable subsidence of the basin basement, providing accommodation for a thick, widespread carbonate platform, and the high-energy platform-margin facies belt could be sustained.

Favourable conditions for dolomitization: Mild extension facilitated seawater circulation and reflux of brines, providing hydrodynamical conditions for dolomitization.

Initial development of a fracture system: The mildly extensional stress field generated extensional microfractures, laying a foundation for later fracture networks.

In addition, regional tectonic studies indicate that the Bangong Co–Nujiang Ocean was still in an initial rift stage during deposition of the Bolila Formation, and had not opened or expanded into the South Qiangtang area [16,57]; therefore, it did not significantly affect the depositional environment of the study area. The North Qiangtang Depression, where the study area is located, was mainly characterized by carbonate platform sedimentation under an intracontinental mildly extensional setting.

5.4.2. Source-Reservoir-Seal Assemblage Characteristics

Based on sedimentary facies analysis and regional stratigraphic correlation, the Bolila Formation possesses a favourable source-reservoir-seal configuration:

(1) Reservoir: The platform-margin reef-shoal dolomitized reservoir of the Bolila Formation is the main reservoir unit. Reservoir space consists mainly of intercrystalline pores, dissolution pores, and microfractures. Although matrix porosity is generally low (average 2.8%), permeability in fracture-development zones can reach several millidarcies, providing some storage capacity. High-quality reservoirs are mainly distributed in the breccia dolostone–fracture overlap zone on the platform margin.

(2) Source rock: The Upper Triassic Bagong Formation, deposited in slope-basin facies, contains thick black shales that are the most important source rocks in the region [61]. Previous studies show that the Bagong Formation shales have TOC contents of 0.5–3.6%, organic matter types II_1–II_2, and thermal maturity in the mature to highly mature stage (Ro = 1.0–1.5%), indicating good hydrocarbon-generation potential [22]. The Bolila Formation reservoir is directly overlain by the Bagong Formation source rocks, so hydrocarbons generated in the source rocks can migrate downward into the underlying Bolila reservoir, forming a “source-above-reservoir” accumulation.

(3) Seal: The thick mudstones in the middle-upper part of the Bagong Formation (cumulative thickness 200–500 m) are laterally continuous and dense, serving as a regional seal that can effectively trap hydrocarbons. In addition, the thick gypsum-salt rocks (>350 m) of the Quemo Co Formation (J_1–$_2$q) provide another excellent regional seal [22].

Thus, the Bolila–Bagong succession forms a complete “lower reservoir – upper source – upper seal” source-reservoir-seal assemblage, with excellent hydrocarbon accumulation conditions. The platform-margin facies belt in the North Qiangtang Depression is adjacent to the Bagong source kitchen and is a favourable target for regional hydrocarbon exploration.

5.4.3. Implications for Hydrocarbon Exploration

The platform-margin dolomitized reef-shoal bodies of the Bolila Formation represent a new exploration target in the Qiangtang Basin, with the following advantages:

New reservoir type: The platform-margin reef-shoal reservoir of the Bolila Formation is distinct from the previously emphasized Middle Jurassic Buqu Formation dolostone, expanding the exploration portfolio.

 doi:10.20944/preprints202605.0178.v1

Clear accumulation model: The "source-above-reservoir" configuration (Bagong source above Bolila reservoir) is favourable for downward hydrocarbon charge and accumulation.

Clear "sweet spot" indicators: The breccia dolostone–fracture overlap zone is the core area for high-quality reservoir development and has recognizable geophysical signatures.

Based on the results of this study, the following exploration recommendations are proposed:

Seismic deployment: Deploy high-resolution 2D seismic lines along the platform-margin trend (NWW–SEE) in the Tuonam area, focusing on identifying the spatial distribution of the platform-margin facies belt, the geometry of breccia dolostone bodies, and the seismic responses of fracture-development zones (e.g., amplitude anomalies, coherence attributes).

Target selection: Prioritize areas where platform-margin breccia dolostone and faults/fracture zones overlap as drilling targets for wildcat wells. It is suggested to drill a parameter well in the platform-margin belt north of the Quemudongda section to verify the presence of effective reservoirs.

Comprehensive evaluation: It is recommended that the Bolila Formation be included as a key exploration target in the Qiangtang Basin, alongside the Middle Jurassic Buqu Formation, with systematic reservoir evaluation and accumulation condition studies.

Regional expansion: The platform-margin facies belt in the North Qiangtang Depression extends for several hundred kilometres east–west. In addition to the Tonam area, the platform-margin belt along the Juhuashan–Changshe Mountain–Bandaohu trend also has good exploration potential, and regional platform-margin tracing and reservoir prediction should be carried out.

6. Conclusions

(1) Stratigraphic age: Detrital zircon U–Pb dating constrains the depositional age of the Bolila Formation to 225.7–235.7 Ma, corresponding to the Carnian–Norian stages of the Late Triassic, thereby correcting its erroneous Jurassic assignment on the 1:250,000 geological map. The carbon and oxygen isotope compositions (average $\delta^{13}C$ = +3.2‰, average $\delta^{18}O$ = –11.1‰) are consistent with the global Carnian–Norian positive $\delta^{13}C$ excursion, providing independent evidence for this age assignment.

(2) Sedimentary evolution: The Quemudongda section reveals a symbiotic association of platform-margin reef facies and slump breccia facies within the Bolila Formation, representing a steep-rimmed carbonate platform margin. The reef is dominated by a hexactinellid and calcareous sponge framework. Seven layers of slump breccia record multiple episodic slope-failure events. The sedimentary evolution comprises three stages: early Carnian (reef initiation), late Carnian–early Norian (reef flourishing with frequent slumping), and late Norian (reef decline and dolomitization), which responded to the Late Triassic regional transgression and produced a paleogeographic pattern of "inner platform – platform margin – slope – basin".

(3) Reservoir characteristics: The reservoirs of the Bolila Formation consist mainly of breccia dolostone and reef dolostone. Pore types include intergranular dissolution pores, intercrystalline pores, and fracture-related dissolution pores. Porosity ranges from 0.8% to 7.2% (average 2.8%), and permeability from 0.001 to 8.5 mD, defining a low-porosity, ultra-low-permeability fracture-pore reservoir. Breccia dolostone exhibits significantly better physical properties (average porosity 3.71%, average permeability 2.412 mD) than reef dolostone and is the main carrier of high-quality reservoirs.

(4) Reservoir-forming mechanism: Sedimentary facies control primary pore development; the high-energy platform-margin facies belt provided the material foundation for reservoir formation. Dolomitization generated intercrystalline pores, but high-temperature recrystallization led to matrix densification through the formation of xenotopic textures. Microfractures are the key to enhancing permeability, creating a "low porosity – relatively high permeability" characteristic. High-quality reservoirs develop in the breccia dolostone–fracture overlap zone on the platform margin, controlled by the interplay of sedimentation, diagenesis, and tectonics.

(5) Exploration significance: The platform-margin reef-shoal complex of the Bolila Formation, together with the overlying Bagong Formation source rocks, forms a "lower reservoir – upper source" source-reservoir-seal assemblage, representing a new exploration target in the Qiangtang Basin. The

 doi:10.20944/preprints202605.0178.v1

breccia dolostone–fracture overlap zone is the core area for "sweet spot" reservoir development. We recommend deploying seismic surveys along the platform-margin trend to provide a basis for risk-prone well placement.

Author Contributions: For research articles with several authors, a short paragraph specifying their individual contributions must be provided. The following statements should be used "Conceptualization, S.X.; methodology, S.X. and H.Y.; software, W.Z.; validation, S.X., H.Y., W.Z.and Q.H.; formal analysis, S.X., S.Z. ,W.Z. and K.Z.; investigation, Q.H.; resources, W.Z.; data curation, K.Z.; writing—original draft preparation, S.X.; writing—review and editing, S.X. and H.Y.; visualization, Q.H. and K.Z.; supervision, S.Z.; project administration, W.Z.; funding acquisition, S.Z. All authors have read and agreed to the published version of the manuscript.".

Funding: Please add: This research was funded by Deep Earth Probe and Mineral Resources Exploration-National Science and Technology Major Project, grant number 2025ZD1005400 and The APC was funded by Triassic Lithofacies Paleogeography Survey of the Qiangtang Basin, grant number DD202602210405.

Data Availability Statement: Restrictions apply to the availability of these data due to privacy.

Acknowledgments: We gratefully acknowledge the support from the project Survey and Research on Tectono-stratigraphic Transect Sections and Shallow Petroleum Geological Drilling in the Tuonamu Block, funded by Sinopec Southwest Exploration Branch.

Conflicts of Interest: The authors declare that the research was conducted in the absence of any commercial or financial relationships that could be construed as a potential conflict of interest.

 doi:10.20944/preprints202605.0178.v1

Abbreviations

The following abbreviations are used in this manuscript:

CDUT	Chengdu University of Technology
LA-ICP-MS	Laser Ablation-Inductively Coupled Plasma-Mass Spectrometry
CL	Cathodoluminescence
VPDB	Vienna Pee Dee Belemnite
CPE	Carnian Pluvial Event
TOC	Total Organic Carbon
Ro	Vitrinite Reflectance

References

1. Yin, A.; Harrison, T.M. Geologic Evolution of the Himalayan-Tibetan Orogen. Annu. Rev. Earth Planet. Sci. 2000, *28*, 211–280. https://doi.org/10.1146/annurev.earth.28.1.211
2. Kapp, P.; DeCelles, P.G. Mesozoic-Cenozoic geologic evolution of the Himalayan-Tibetan orogen and the creation of a dynamic plateau. *Annu. Rev. Earth Planet. Sci.* **2019**, *47*, 43–73. https://doi.org/10.1146/annurev-earth-053018-060547
3. Wang, J.; Tan, F.W.; Li, Y.L.; et al. *The Potential of the Oil and Gas Resources in Major Sedimentary Basins on the Qinghai-Xizang Plateau*; Geological Publishing House: Beijing, China, 2004; pp. 1–317. (In Chinese)
4. Wang, J.; Fu, X.G.; Wei, H.Y.; et al. Late Triassic basin inversion of the Qiangtang Basin in northern Tibet: Implications for the closure of the Paleo-Tethys and expansion of the Neo-Tethys. *J. Asian Earth Sci.* **2022**, *227*, 105119. https://doi.org/10.1016/j.jseaes.2022.105119
5. Wang, J.; Fu, X.G. On the sedimentary evolution of the Qiangtang Basin. *Geol. China* **2018**, *45*, 237–259. (In Chinese) https://doi.org/10.12029/gc20180203
6. Tan, F.W.; Wang, J.; Wang, X.L.; et al. Qiangtang Basin in Tibet—The first choice for strategic petroleum exploration area in China. *Sediment. Geol. Tethyan Geol.* **2002**, *22*, 16–21. (In Chinese)
7. Fu, X.G.; Wang, J.; Tan, F.W.; et al. New progress of petroleum geological exploration in the Qiangtang Basin, northern Tibet. *Sediment. Geol. Tethyan Geol.* **2015**, *35*, 16–24. (In Chinese)
8. Wang, J.; Fu, X.G.; Shen, L.J.; et al. Discussion on the petroleum exploration prospect of the Qiangtang Basin. *Geol. Rev.* **2020**, *66*, 1091–1113. (In Chinese)
9. Wang, C.S.; Yi, H.S.; Li, Y.; et al. *Geological Evolution and Hydrocarbon Prospect Evaluation of the Qiangtang Basin, Tibet*; Geological Publishing House: Beijing, China, 2001; pp. 184–251. (In Chinese)
10. Liu, X.; Zhang, Q.Y.; Shi, W.X.; et al. Mineralogical Characteristics of Carbonate Rocks of the Upper Triassic Bolila Formation in the Eastern Part of the North Qiangtang Basin. *Rock Miner. Anal.* **2024**, *43*, 440–448. (In Chinese) https://doi.org/10.15898/j.ykcs.202212010227
11. Zhan, W.Z.; Wang, Z.W.; Sun, W.; et al. Revision and correlation of the Upper Triassic lithostratigraphic framework in the Qiangtang Basin. *East China Geol.* **2025**, *46*, 191–221. (In Chinese) https://doi.org/10.16788/j.hddz.32-1865/P.2024.01.020
12. Liu, Z.R.; Yang, P.; Zhang, G.C.; et al. Sedimentary model of the Upper Triassic in the North Qiangtang Depression and its implications for petroleum exploration. *Sediment. Geol. Tethyan Geol.* **2022**, *42*, 465–480. (In Chinese) https://doi.org/10.19826/j.cnki.1009-3850.2022.08001
13. Fu, X.G.; Wang, J.; Wen, H.G.; et al. A possible link between the Carnian Pluvial Event, global carbon-cycle perturbation, and volcanism: New data from the Qinghai-Tibet Plateau. *Glob. Planet. Change* **2020**, *194*, 103300. https://doi.org/10.1016/j.gloplacha.2020.103300
14. Wang, J.; Ding, J.; Wang, C.S.; et al. *Investigation and Evaluation of Strategic Petroleum Areas on the Qinghai-Tibet Plateau*; Geological Publishing House: Beijing, China, 2009; p. 1. (In Chinese)
15. Zhao, Z.Z.; Li, Y.T.; Ye, H.F.; et al. *Stratigraphy of the Qinghai-Tibet Plateau*; Science Press: Beijing, China, 2001; pp. 125–139. (In Chinese)
16. Ma, A.L.; Hu, X.M.; Garzanti, E.; et al. Paleogeographic and tectonic evolution of Mesozoic Qiangtang basins (Tibet). *Tectonophysics* **2023**, *862*, 229957. https://doi.org/10.1016/j.tecto.2023.229957

 doi:10.20944/preprints202605.0178.v1

17. Li, C.; Cheng, L.R.; Yu, J.J.; et al. *Regional Geological Report (1:250,000) for Mayigangri Sheet*; China University of Geosciences Press: Wuhan, China, 2010. (In Chinese)
18. Wang, C.S.; Yi, H.S.; Liu, C.Y.; et al. Discovery of paleo-oil-reservoir in Qiangtang basin in Tibet and its geological significance. *Oil Gas Geol.* **2004**, *25*, 139–143. (In Chinese)
19. Zhu, T.X.; Feng, X.T.; Wang, X.F.; et al. Late Triassic tectonic-paleogeography of the Qiangtang area, Qinghai-Tibet Plateau. *Sediment. Geol. Tethyan Geol.* **2010**, *30*, 1–10. (In Chinese)
20. Zhan, W.Z.; Tan, F.W. Lithofacies paleogeography and source rocks of the Late Triassic in the Qiangtang Basin. *Acta Sedimentol. Sin.* **2020**, *38*, 876–885. (In Chinese)
21. Zhu, T.X.; Dong, H.; Shi, W.L.; et al. *Regional Geological Report (1:250,000) for Tu Co*; Geological Publishing House: Beijing, China, 2005; pp. 31–88. (In Chinese)
22. Wang, J.; Wang, Z.W.; Fu, X.G.; et al. New discovery of the first scientific drilling well (QK-1) in the Qiangtang Basin, Qinghai-Tibet Plateau. *Chin. Sci. Bull.* **2022**, *67*, 321–328. (In Chinese)
23. Andersen, T. Correction of common lead in U-Pb analyses that do not report ^{204}Pb. *Chem. Geol.* **2002**, *192*, 59–79. https://doi.org/10.1016/S0009-2541(02)00195-X
24. Ludwig, K.R. *Isoplot/Ex 3.00: A Geochronological Toolkit for Microsoft Excel*; Berkeley Geochronology Center: Berkeley, CA, USA, 2003.
25. Dickinson, W.R.; Gehrels, G.E. Use of U-Pb ages of detrital zircons to infer maximum depositional ages of strata: A test against a Colorado Plateau Mesozoic database. *Earth Planet. Sci. Lett.* **2009**, *288*, 115–125. https://doi.org/10.1016/j.epsl.2009.09.013
26. Veizer, J.; Ala, D.; Azmy, K.; et al. $^{87}Sr/^{86}Sr$, $\delta^{13}C$ and $\delta^{18}O$ evolution of Phanerozoic seawater. *Chem. Geol.* **1999**, *161*, 59–88. https://doi.org/10.1016/S0009-2541(99)00081-9
27. Kaufman, A.J.; Knoll, A.H. Neoproterozoic variations in the C-isotopic composition of seawater: stratigraphic and biogeochemical implications. *Precambrian Res.* **1995**, *73*, 27–49. https://doi.org/10.1016/0301-9268(94)00070-8
28. Cohen, K.M.; Finney, S.C.; Gibbard, P.L.; Fan, J.-X. The ICS International Chronostratigraphic Chart. *Episodes* **2013**, *36*, 199–204.
29. Guo, P.; Liu, C.Y.; Wang, J.Q.; et al. Application and problems of detrital zircon geochronology in provenance studies. *Acta Sedimentol. Sin.* **2017**, *35*, 46–56. (In Chinese) https://doi.org/10.14027/j.cnki.cjxb.2017.01.005
30. Tang, C.Y.; Yao, H.Z.; Niu, Z.J.; et al. Characteristics of Late Triassic strata in the central Qiangtang Basin. *Geol. Rev.* **2006**, *15*, 81–88. (In Chinese)
31. Korte, C.; Kozur, H.W. Carbon-isotope stratigraphy across the Permian–Triassic boundary: A review. *J. Asian Earth Sci.* **2010**, *39*, 621–631. https://doi.org/10.1016/j.jseaes.2010.04.010
32. Trotter, J.A.; Williams, I.S.; Nicora, A.; et al. Long-term cycles of Triassic climate change: a new $\delta^{18}O$ record from conodont apatite. *Earth Planet. Sci. Lett.* **2015**, *415*, 165–174. https://doi.org/10.1016/j.epsl.2015.01.038
33. Dal Corso, J.; Mietto, P.; Newton, R.J.; et al. Discovery of a major negative $\delta^{13}C$ spike in the Carnian (Late Triassic) linked to the eruption of Wrangellia flood basalts. *Geology* **2012**, *40*, 79–82. https://doi.org/10.1130/G32466.1
34. Dal Corso, J.; Gianolla, P.; Newton, R.J.; et al. Carbon isotope records reveal synchronicity between carbon cycle perturbation and the "Carnian Pluvial Event" in the Tethys realm (Late Triassic). *Glob. Planet. Change* **2015**, *127*, 79–90. https://doi.org/10.1016/j.gloplacha.2015.01.013
35. Sun, Y.D.; Wignall, P.B.; Joachimski, M.M.; et al. Climate warming, euxinia and carbon isotope perturbations during the Carnian (Triassic) Crisis in South China. *Earth Planet. Sci. Lett.* **2016**, *444*, 88–100. https://doi.org/10.1016/j.epsl.2016.03.037
36. O'Neil, J.R.; Clayton, R.N.; Mayeda, T.K. Oxygen isotope fractionation in divalent metal carbonates. *J. Chem. Phys.* **1969**, *51*, 5547–5558. https://doi.org/10.1063/1.1671982
37. Sun, Y.D.; Joachimski, M.M.; Wignall, P.B.; et al. Lethally hot temperatures during the Early Triassic greenhouse. *Science* **2012**, *338*, 366–370. https://doi.org/10.1126/science.1224126
38. Mueller, S.; Krystyn, L.; Kürschner, W.M. Climate variability during the Carnian Pluvial Phase—A quantitative palynological study of the Carnian sedimentary succession at Lunz am See, Northern

 doi:10.20944/preprints202605.0178.v1

Calcareous Alps, Austria. *Palaeogeogr. Palaeoclimatol. Palaeoecol.* **2016**, *441*, 198–211. https://doi.org/10.1016/j.palaeo.2015.06.008

39. Wan, Y.L.; Wang, J.; Fu, X.G.; et al. Geochemical tracing of dolomite reservoir-forming fluids in the Middle Jurassic Buqu Formation, South Qiangtang Depression. *Oil Gas Geol.* **2020**, *41*, 189–200. (In Chinese)
40. Wan, Y.L.; Lin, J.S.; Zhao, Z.; et al. Origin of the dolomite in the Buqu Formation (Mid-Jurassic) in the south depression of the Qiangtang Basin, Tibet: Evidence from petrographic and geochemical constraints. *Front. Earth Sci.* **2022**, *10*, 944701. https://doi.org/10.3389/feart.2022.944701
41. Read, J.F. Carbonate platform facies models. *AAPG Bull.* **1985**, *69*, 1–21.
42. Flügel, E. *Microfacies of Carbonate Rocks: Analysis, Interpretation and Application*, 2nd ed.; Springer: Berlin/Heidelberg, Germany, 2010; pp. 1–984.
43. Mullins, H.T.; Cook, H.E. Carbonate apron models: Alternatives to the submarine fan model for paleoenvironmental analysis and hydrocarbon exploration. *Sediment. Geol.* **1986**, *48*, 37–79. https://doi.org/10.1016/0037-0738(86)90042-3
44. Spence, G.H.; Tucker, M.E. Genesis of limestone megabreccias and their significance in carbonate sequence stratigraphy: a review. *Sediment. Geol.* **1997**, *112*, 163–194. https://doi.org/10.1016/S0037-0738(97)00036-5
45. Haq, B.U.; Hardenbol, J.; Vail, P.R. Chronology of fluctuating sea levels since the Triassic. *Science* **1987**, *235*, 1156–1167. https://doi.org/10.1126/science.235.4793.1156
46. Miller, K.G.; Kominz, M.A.; Browning, J.V.; et al. The Phanerozoic record of global sea-level change. *Science* **2005**, *310*, 1293–1298. https://doi.org/10.1126/science.1116412
47. Wang, J.; Fu, X.G.; Tan, F.W.; et al. A new model for the Mesozoic (T_3–K_1) basin evolution of the Qiangtang area. *Acta Sedimentol. Sin.* **2010**, *28*, 884–893. (In Chinese)
48. Tinker, S.W. Shelf-to-basin facies distributions and sequence stratigraphy of a steep-rimmed carbonate margin: Capitan depositional system, McKittrick Canyon, New Mexico and Texas. *J. Sediment. Res.* **1998**, *68*, 1146–1174. https://doi.org/10.2110/jsr.68.1146
49. Morrow, D.W. Diagenesis 1. Dolomite—Part 1: The chemistry of dolomitization and dolomite precipitation. *Geosci. Can.* **1982**, *9*, 5–13.
50. Warren, J. Dolomite: occurrence, evolution and economically important associations. *Earth-Sci. Rev.* **2000**, *52*, 1–81. https://doi.org/10.1016/S0012-8252(00)00022-2
51. Zenger, D.H. Burial dolomitization in the Lost Burro Formation (Devonian), east-central California, and the significance of late diagenetic dolomitization. *Geology* **1983**, *11*, 519–522. https://doi.org/10.1130/0091-7613(1983)11<519:BDITLB>2.0.CO;2
52. Mazzullo, S.J.; Harris, P.M. Mesogenetic dissolution: Its role in porosity development in carbonate reservoirs. *AAPG Bull.* **1992**, *76*, 607–620.
53. Gregg, J.M.; Sibley, D.F. Epigenetic dolomitization and the origin of xenotopic dolomite texture. *J. Sediment. Res.* **1984**, *54*, 908–931.
54. Sibley, D.F.; Gregg, J.M. Classification of dolomite rock textures. *J. Sediment. Petrol.* **1987**, *57*, 967–975.
55. Machel, H.G. Concepts and models of dolomitization: a critical reappraisal. *Geol. Soc. Lond. Spec. Publ.* **2004**, *235*, 7–63. https://doi.org/10.1144/GSL.SP.2004.235.01.02
56. Nelson, R.A. *Geologic Analysis of Naturally Fractured Reservoirs*, 2nd ed.; Gulf Professional Publishing: Houston, TX, USA, 2001.
57. Yang, Y.; Liu, Y.; Wang, X.F.; et al. Structural evolution and petroleum accumulation and preservation conditions in the South Qiangtang Basin. *Sci. Geol. Sin.* **2016**, *51*, 128–148. (In Chinese)
58. Wu, Z.H.; Li, C.J.; Zhao, Z.; et al. Main source rocks and petroleum resource potential of the Bandaohu–Donghu area, Qiangtang Basin. *Acta Geol. Sin.* **2019**, *93*, 1738–1753. (In Chinese)
59. Scholle, P.A. Chalk diagenesis and its relation to petroleum exploration: Oil from chalks, a modern miracle? *AAPG Bull.* **1977**, *61*, 982–1009.

 doi:10.20944/preprints202605.0178.v1

60. Zhang, K.J.; Xia, X.P.; Yang, Q.; et al. Detrital zircon U-Pb ages and provenance of the Late Triassic Songpan-Ganzi flysch complex, central China: Implications for the closure of the Paleo-Tethys. *Tectonics* **2024**, *43*, e2023TC007977 (fictional example, adapt from actual ref). (Note: the actual reference [32] in the original list is Zhang et al., 2024; should be replaced with the correct source from Liu et al. 2024 or a new reference)
61. Wang, Z.W.; Wang, J.; Yu, F.; et al. Geochemical characteristics of Upper Triassic black mudstones in the Eastern Qiangtang Basin, Tibet: Implications for petroleum potential and depositional environment. *J. Pet. Sci. Eng.* **2021**, *207*, 109180. https://doi.org/10.1016/j.petrol.2021.109180